Study on the Mix Design and Performance of High Strength Fluid Curing Soil Prepared with Redundant Soil

Li Zhanguo, Guo Ziyi, Zhou Yongxiang, Zhang Renjie, Chen Ying
School of Civil Engineering, Beijing University of Technology, Beijing, China

Abstract: High-strength fluid-cured soil can be used as a new type of pile foundation material for pressure-type composite anti-pull piles, significantly enhancing the seismic performance of pile foundations and effectively addressing the issue of buoyancy resistance. The study focuses on preparing curing agents primarily from slag powder, steel slag powder, and desulfurization gypsum, mixed with excess construction waste soil to investigate their mechanical properties and micro-mechanisms. Results show that the optimal ratio is slag powder: steel slag powder: gypsum: alkaline activator = 60:13:14:13, with a water-to-curing agent ratio of 0.32. Compared to cement soil, this material offers advantages such as higher strength, lower cost, and reduced carbon emissions, with its compressive strength increasing with the addition of curing agent. Analysis of specimen size effects indicates that the strength of a 40mm × 40mm × 160mm prism is 1.1 to 1.15 times that of a 70.7mm cube and 1.2 to 1.25 times that of a 50mm × 100mm cylinder. Additionally, the self-shrinkage rate of this material is lower than that of cement soil, and it can exhibit slight expansion with increasing curing agent content. Microscopic mechanisms reveal that a multi-component composite curing agent reduces porosity and generates more calcium sulfoaluminate, thereby enhancing material strength.

Keywords: Flow Curing Soil; Solid Waste; Self-Shrinkage; Strength; Microstructure

1. Introduction

As China's urbanization process accelerates, urban land resources have become increasingly scarce. The number of underground structures such as basements of high-rise buildings, underground shopping malls, and subterranean transportation systems is growing, with their depth increasing and area expanding. The issue of buoyancy resistance has also become more prominent[1-2]. In practical engineering applications, the most commonly used and reliable method for addressing buoyancy resistance is the use of anti-pull piles or anti-floating anchor rods [3]. Pressure-type anti-pull piles are expansion anchor piles with an "expanded anchoring end," where the pile body is in a "pressurized expansion" state. Compared to non-pressure-type anti-pull piles, they start to bear loads from the bottom of the pile, effectively mobilizing deep soil [4]. However, in actual engineering practice, single-pile methods often fail to meet engineering requirements. As a new foundation treatment technology, reinforced composite piles [5-6] have been widely applied in recent engineering practices. The construction process involves implanting high-strength concrete core piles concentrically inside the cement-soil mixing piles before they begin to set, forming a composite pile structure. This composite pile not only significantly increases the actual friction surface of the pile but also effectively enhances its compressive strength. Research by Qian Yujun et al. [7] shows that cement-soil reinforced composite piles outperform traditional concrete pipe piles in terms of load-bearing capacity, construction efficiency, and economic benefits. Dong et al. [8] found through on-site load tests of reinforced cement-soil mixing piles that the characteristic value of bearing capacity has significantly improved compared to cement mixing composite pile foundations. Related studies show that the pressure-type composite anti-pull pile combined with cement soil composite pipe pile has obvious advantages in dealing with the problem of underground structure floating, especially in the application scenarios where the anti-floating water level is high or the pipe pile is difficult to be driven into the bottom layer due to dense sand.

Cement soil, as the foundation material for pressure-type composite uplift piles, is widely used in various engineering scenarios due to its

abundant sources. Relevant scholars have conducted extensive research on the properties of cement soil. Tang Yixin et al. [9] pointed out through unconfined compression tests that the strength of cement soil mainly depends on the amount of cement added, which is consistent with the conclusions drawn by Lee et al. [10] and Fischer et al. [11]. Khattak et al. [12] proposed that the more cement added to cement soil, the greater its shrinkage, affecting the frictional resistance between cement soil and rock walls. Additionally, the uniformity of cement soil mixing piles underground remains a challenging issue. Therefore, using pre-mixed fluid-cured soil as an alternative to cement mixing piles can effectively address the homogeneity of cured soil. Fluid-cured soil is currently mainly used for backfilling projects, with a strength generally ranging from 0.3 to 1MPa [13]. However, as a foundation material, it requires higher strength. Analysis suggests that fluid-cured soil with an unconfined compressive strength of 4-5MPa can significantly enhance the load-bearing capacity and buoyancy resistance of reinforced composite piles. At the same time, as a foundation material, it will open up new fields for the extended application of fluid-cured soil technology [14]. Zhou Yongxiang et al. [13]'s research indicates that in fluid-cured soil systems with high water content, the technical and economic advantages of cement are not significant, making it difficult to meet the requirements of new pile methods combining pressure-type uplift piles and cement soil composite pipe piles. Increasing the amount of cement added would substantially increase project costs and shrinkage. In addition, the production of cement consumes a large amount of non-renewable resources and produces a large amount of greenhouse gas emissions [15].
Considering the needs of economic and environmental protection, cement reinforcement is less effective than curing agents primarily composed of volcanic ash materials such as slag powder [16]. If industrial solid waste can be utilized to prepare high-strength fluidized curing soil, it not only enhances the performance of the curing soil and reduces engineering costs but also alleviates environmental burdens [17-19]. In light of this, this paper uses industrial solid wastes such as slag powder, steel slag powder, and desulfurization gypsum, along with redundant construction waste, to prepare high-strength fluidized curing soil. First, the optimal mix ratio of high-strength fluidized curing soil is determined through orthogonal compound design methods, and the effects of different specimen sizes and curing agent dosages on the compressive strength of high-strength fluidized curing soil are investigated. The self-shrinkage test is used to explore the impact of multiple composite curing agent dosages on the self-shrinkage of high-strength fluidized curing soil. Finally, scanning electron microscopy and mercury porosimetry are employed to investigate the curing mechanism of the soil using multiple composite curing agents.

2. Materials and Test Methods

2.1 Test Materials

The soil samples were collected from a construction waste disposal site in Changping District, Beijing, as redundant soil during the crushing process of demolition waste. The chemical composition is shown in Table 1. Before testing, the soil was air-dried and sieved through a 2.36mm aperture to be stored for later use. The particle size distribution is illustrated in Figure 1. Cement used is PO42.5 grade, with physical properties indicated in Table 2. The chemical compositions of slag powder, steel slag powder, and desulfurization gypsum are also shown in Table 2. Water for mixing is tap water.

Table 1. Basic Characteristics of Natural River Sand

chemical composition	mass fraction /%								
	SiO2	Al2O3	Fe2O3	CaO	MgO	Na2O	K2O	SO3	else
soil sample	52.67	15.45	5.93	15.03	3.60	1.53	2.90	1.27	1.62
ground slag	28.89	14.75	0.67	38.41	9.53	1.06	0.64	2.81	3.24
Steel powder	18.55	7.48	12.70	45.67	4.85	0.34	0.17	1.10	9.14
Desulphurized gypsum	1.14	0.44	0.19	45.30	0.80	0.05	0.07	50.63	1.32

Table 2. Cement Physical Properties

fineness	density	normal consistency	time of setting/min		rupture strength /MPa		compression strength/MPa	
/(m2/kg)	/(kg/m3)	water consumption /%	initial set	final set	3d	28d	3d	28d
335	3120	26.1	204	267	5.5	9.8	27.3	54.2

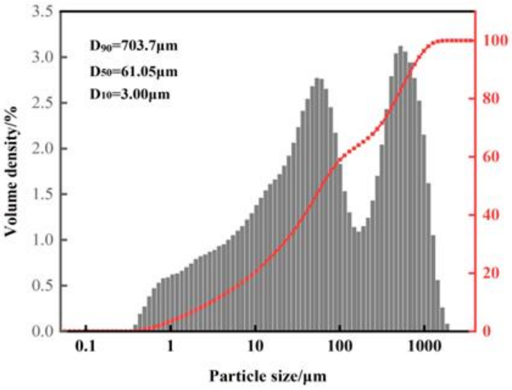

Figure1. Particle Size Distribution of Redundant Soil

2.2 Sample Preparation

Mix cement or composite curing agent with water in proportion, and stir evenly with a mixer. Then pour the soil into it, stir for 2min, and pour it into molds of different types. Then demold and put it in a standard curing box to cure at the corresponding age.

2.3 Test Method

Compressive strength test: The test method is referred to GB/T 17671-2021 "Cement mortar strength inspection method (ISO method)", and the test instrument is universal testing machine (model SHT4605).

Flow Test: This experiment uses the flow test according to the American Society for Testing and Materials (ASTM) standard ASTM D6103/D6103M. The test apparatus consists of a plastic cylinder with an opening at both ends, measuring 75mm in diameter and 150mm in height (see Figure 2). The specific procedure involves placing the test cylinder on a smooth glass plate, filling it quickly with freshly mixed fluid-cured soil, and then lifting it to allow the fluid-cured soil to freely spread on the glass plate. When the flow of the fluid-cured soil ceases, measure the diameter of the circular disk formed in both orthogonal directions, and take the average value as the flowability.

Self-contraction Test: This paper employs a corrugated tube to measure self-contraction, where freshly mixed material is injected into a flexible corrugated tube, sealed at both ends, and placed in a constant temperature environment. Axial length changes are monitored in real-time using displacement sensors or micrometers. This method effectively avoids external constraints and accurately reflects the self-contraction characteristics caused by hydration reactions.

Scanning electron microscope test: the instrument produced by FEI Company of the United States is used, model Quanta FEG 250, acceleration voltage is 200V-30KV.

Mercury pressure test: mercury pressure meter of model AutoPore IV 9510 is used. The pressure range of the instrument is 0.50psia-60000psia, and the aperture range is 0.003μm~360μm.

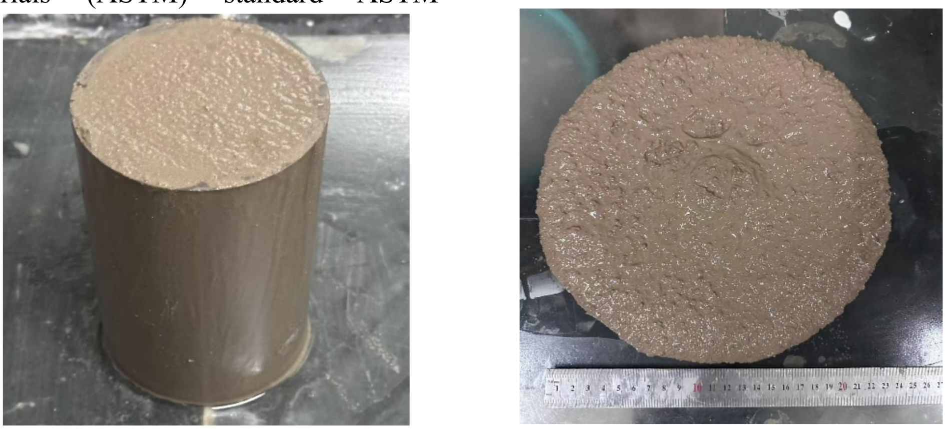
Figure 2. Computer Automatic Cement Bending and Compression Testing Machine

3. Orthogonal Mix Design and Result Analysis

3.1 Orthogonal Mix Design Scheme and Test Results

According to the results of preliminary binary/trinary exploratory experiments: when slag, steel slag, gypsum, and alkaline activator are combined in appropriate proportions, different characteristics of solid waste can play roles at different stages of hydration and structure formation, achieving complementary advantages. The orthogonal experiment selected three factors that have significant impacts on flowability, 7-day strength, and 28-day strength: gypsum dosage, alkaline activator dosage, and water-to-solid ratio. Each factor was set at three levels, using the L9(3^4) orthogonal experiment, with flowability, 7-day strength, and 28-day strength as evaluation indicators to determine the optimal mix ratio.

The test results show that when the gypsum content is between 10% to 18%, the alkaline activator content is between 11% to 15%, and the water-to-solid ratio is between 1.29 and 0.35, with an optimal slag content of 60%, the performance is best. The orthogonal experimental design scheme is as follows: the gypsum content is set at 10%,14%, and 18%; the alkaline activator content is set at 11%,13%, and 15%; the steel slag content is supplemented to 100% based on the first two; the slag content is set at 60%. The orthogonal experimental factors and levels are shown in Table 3. According to the orthogonal design table in Table 3, the experiment was conducted, and the results are presented in Table 4.

Table 3. Orthogonal Experimental Factors and Horizontal Design

factor	horizontal		
	1	2	3
A-gyp (%)	10	14	18
B-basic activator (%)	11	13	15
C water solid ratio	0.29	0.32	0.35

Table 4. Orthogonal Experimental Scheme and Results

test number	factor			evaluating indicator		
	A-gyp	B-basicity booster	C water solid ratio	mobility /mm	7d intensity /MPa	28d strength /MPa
1	1	1	1	225	4.28	6.42
2	1	2	3	265	4.25	6.45
3	1	3	2	245	4.62	7.05
4	2	1	3	270	3.28	6.48
5	2	2	2	230	4.92	8.54
6	2	3	1	205	5.25	7.12
7	3	1	2	255	3.76	7.92
8	3	2	1	205	4.85	7.87
9	3	3	3	260	3.48	6.05

3.2 Analysis of Variance of Orthogonal Test Results

In orthogonal experimental analysis, Ki represents the sum of the test index values at the i-th level of the corresponding factor, ki indicates the mean value of the test index at the i-th level of the corresponding factor, and r represents the difference between the maximum and minimum values of ki in the fixed factors. The larger the r value, the greater the impact of different levels of this factor on the evaluation index, indicating that this factor has a greater influence on the evaluation index. Conversely, it suggests that this factor has a smaller impact on the experimental results.

Through orthogonal analysis of flowability, the analysis of the range of variation (r values) in Table 5 shows that the three factors affect flowability in the following order: C> B> A, i.e., water-to-solid ratio> alkaline activator> gypsum. With a flowability target of 220-240 mm^2/s^2, the optimal conditions for flowability are determined from the magnitudes of k1, k2, and k3 to be A2B2C2. The analysis of the range of variation (r values) in Table 6 for 7-day strength shows that the three factors affect 7-day strength in the following order: C> A> B, i.e., water-to-solid ratio> gypsum> alkaline activator. With a maximum 7-day strength as the optimization target, the optimal conditions for 7-day strength are determined from the magnitudes of k1, k2, and k3 to be A2B2C1. The analysis of the range of variation (r values) in Table 7 for 28-day strength shows that the three factors affect 28-day strength in the following order: C> B> A, i.e., water-to-solid ratio> alkaline activator> gypsum. With a maximum 28-day strength as the optimization target, the optimal conditions for 28-day strength are determined from the magnitudes of k1, k2, and k3 to be A2B2C2.

Table 5. Results of Range Analysis of Liquidity for Various Factors

	A	B	C
K1	seven hundred and thirty five point zero zero	seven hundred and fifty point zero zero	six hundred and thirty five point zero zero
K2	seven hundred and five point	seven hundred point zero	seven hundred and thirty

	zero zero	zero	point zero zero
K3	seven hundred and twenty point zero zero	seven hundred and ten point zero zero	seven hundred and ninety five point zero zero
k1	two hundred and forty five point zero zero	two hundred and fifty point zero zero	two hundred and eleven point six seven
k2	two hundred and thirty five point zero zero	two hundred and thirty three point three three	two hundred and forty three point three three
k3	two hundred and forty point zero zero	two hundred and thirty six point six seven	two hundred and sixty five point zero zero
r	ten point zero zero	sixteen point six seven	fifty three point three three
Order of influence: C> B> A Best combination: A2B2C2			

Table 6. Results of Range Analysis of Various Factors On 7-Day Intensity

	A	B	C
K1	thirteen point one five	eleven point three two	fourteen point three eight
K2	thirteen point four five	fourteen point zero two	thirteen point three zero
K3	twelve point zero nine	thirteen point three five	eleven point zero one
k1	four point three eight	three point seven seven	four point seven nine
k2	four point four eight	four point six seven	four point four three
k3	four point zero three	four point four five	three point six seven
r	point four five	point nine zero	one point one two
Order of influence: C>B>A Optimal combination: A2B2C1			

Table 7. The results of the range analysis of each factor on 28d strength

	A	B	C
K1	nineteen point nine two	twenty point eight two	twenty one point four one
K2	twenty two point one four	twenty two point eight six	twenty three point five one
K3	twenty one point eight four	twenty point two two	eighteen point nine eight
k1	six point six four	six point nine four	seven point one four
k2	seven point three eight	seven point six two	seven point eight four
k3	seven point two eight	six point seven four	six point three three
r	point seven four	point eight eight	one point five one
Order of influence: C>B>A Optimal combination: A2B2C2			

3.3 Variance Analysis of Orthogonal Test Results

ANOVA was conducted on workability, 7-day strength, and 28-day strength. The results of the ANOVA are shown in Tables 8 to 10. From the ANOVA tables in Tables 8 to 10, it can be seen that gypsum has an extremely significant effect on workability (P<0.01), and alkaline activators have a significant effect on workability (P<0.05). Gypsum and alkaline activators have a significant effect on 7-day strength (P<0.05); gypsum, alkaline activators, and water-to-cement ratio all have a significant effect on 28-day strength (P<0.05).

Table 8. Variance Analysis Results of Each Factor On Mobility

source	quadratic sum	free degree	mean square	F price	P price	conspicuousness
A	one hundred and fifty point zero zero zero	two	seventy five point zero zero zero	nine point zero zero zero	point one zero zero	
B	four hundred and sixty six point six six seven	two	two hundred and thirty three point three three three	twenty eight point zero zero zero	point zero three four	*
C	four thousand three hundred and sixteen point six six seven	two	two thousand one hundred and fifty eight point three three three	two hundred and fifty nine point zero zero zero	point zero zero four	**
error e	sixteen point six six seven	two	eight point three three three			
F0.05(2,2)=19,F0.01(2,2)=99						

Note: ** indicates a highly significant (P <0.01) effect, and * indicates a significant (P <0.05) effect

Table 9. Analysis of Variance Results of Various Factors on 7-Day Intensity

source of variation	quadratic sum	free degree	mean square	F price	P price	conspicuousness

A	point three four zero	two	point one seven zero	five point zero nine three	point one six four	
B	one point three one eight	two	point six five nine	nineteen point seven two zero	point zero four eight	*
C	one point nine seven four	two	point nine eight seven	twenty nine point five four three	point zero three three	*
error e	point zero six seven	two	point zero three three			
F0.05(2,2)=19,F0.01(2,2)=99						

Note: ** indicates a highly significant (P <0.01) effect, and * indicates a significant (P <0.05) effect

Table 10. Analysis of Variance Results of Various Factors on 28 Day Intensity

source of variation	quadratic sum	free degree	mean square	F price	P price	conspicuousness
A	point nine six seven	two	point four eight four	twenty two point two eight six	point zero four three	*
B	one point two seven seven	two	point six three eight	twenty nine point four one nine	point zero three three	*
C	three point four two six	two	one point seven one three	seventy eight point nine four five	point zero one three	*
error e	point zero four three	two	point zero two two			
F0.05(2,2)=19,F0.01(2,2)=99						

Note: ** indicates a highly significant (P <0.01) effect, and * indicates a significant (P <0.05) effect

Considering the impact of three factors on the indicators (flowability, 7-day strength, 28-day strength), it is found that for Factor A, when A is at level 2, flowability reaches its maximum value at k2=235, and both 7-day and 28-day strengths also reach their maximum values. Therefore, A2 is chosen as the optimal level, meaning that when gypsum content is 14%, flowability, 7-day strength, and 28-day strength are all optimal. For Factor B, when B is at level 2, flowability reaches its maximum value at k2=233, and both 7-day and 28-day strengths also reach their maximum values. Therefore, B2 is chosen as the optimal level, meaning that when alkaline accelerator content is 13%, flowability, 7-day strength, and 28-day strength are relatively optimal. For Factor C, 7-day strength reaches its maximum value at level 1, and when C is at level 2, flowability reaches its maximum value at k2=243.33, and 28-day strength also reaches its maximum value. Therefore, C2 is chosen as the optimal level, meaning that when water-to-cement ratio is 0.32, flowability, 7-day strength, and 28-day strength are all optimal. Specifically, when gypsum content is 14%, alkaline accelerator content is 13%, and water-to-cement ratio is 0.32, flowability, 7-day strength, and 28-day strength are all optimal.

3.4 Influence of Different Specimen Size and Curing Agent Dosage on High Strength Flow Curing Soil

The current standards for the size of compression strength specimens for flow-cured soil are not uniform: ACI 229R recommends using cylindrical specimens measuring 150mm × 300mm or with a height-to-diameter ratio of ≥2; DBJ51/T 188-2022 suggests using 70.7mm×70.7mm×70.7mm cubic specimens; while some researchers use prismatic specimens measuring 40mm × 40mm × 160mm. The inconsistency in specimen sizes leads to inconsistent compressive strength results, hindering the promotion and application of flow-cured soil in practical engineering. To study the relationship between compressive strength at different specimen sizes, this paper selects cylindrical specimens measuring 50mm × 100mm (cubic specimens in Figure 3),70.7mm×70.7mm×70.7mm (Figure 4), prismatic specimens measuring 40mm × 40mm × 160mm (Figure 5), and measures their 7d and 28d compressive strengths to explore the relationship between these strengths. Table 11 presents the results of unconfined compressive strength tests for cured soil at 7d and 28d under different sizes and admixture levels. As shown in Table 11, the strength relationship among the three types of specimens is: prismatic> cubic> cylindrical, where the unconfined compressive strength of the 40mm × 40mm × 160mm prismatic specimen is 1.1 to 1.15 times that of the 70.7mm×70.7mm×70.7mm cubic specimen, and the unconfined compressive strength of the 40mm × 40mm × 160mm prismatic specimen is 1.2 to 1.25 times that of the 50mm × 100mm cylindrical specimen.

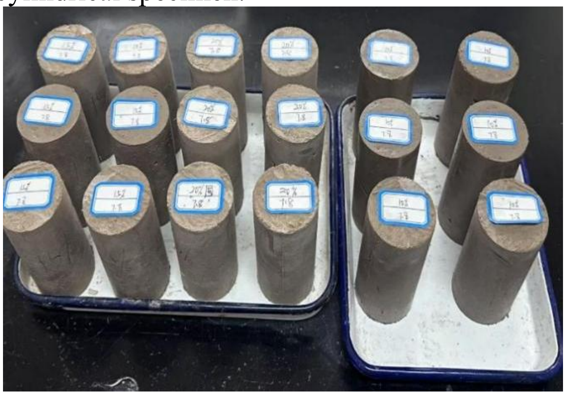

Figure 3. 50mm × 100mm Cylindrical Specimen

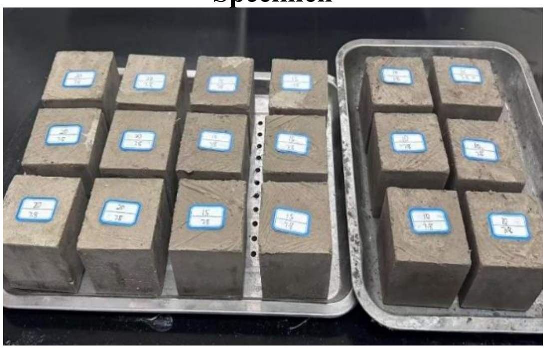

Figure 4. 70.7mm × 70.7mm 70.7mm Cubic Specimen

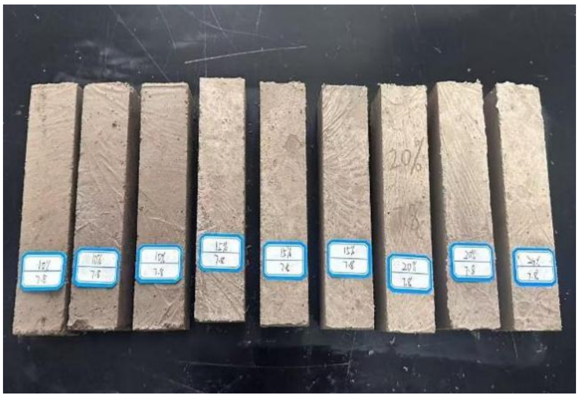

Figure 5. 40mm × 40mm × 160mm Cube Specimen

As shown in Table 11, when the mold type and curing agent dosage are the same, the compressive strength of high-strength flow-cured soil is higher than that of cement soil. By comparing high-strength flow-cured soil with the same mold type, it can be observed that as the dosage of multi-component composite curing agent increases, the strength of high-strength flow-cured soil gradually increases. Taking a mold size of 40mm × 40mm × 160mm as an example, when the dosage of multi-component composite curing agent increases from 10% to 20%, the 7-day compressive strength of high-strength flow-cured soil increases from 1.83MPa to 4.92 MPa, and the 28-day compressive strength increases from 2.77MPa to 8.2 MPa.

Table 11 Compressive strength of stabilized soil

Mold types	Type of curing agent	Curing agent dosage	7d strength /MPa	28d strength /MPa
70.7mm×70.7mm70.7mm	Multifunctional curing agent	10%	1.61	2.40
40mm×40mm×160mm	Multifunctional curing agent		1.83	2.77
50mm×100mm	Multifunctional curing agent		1.51	2.29
70.7mm×70.7mm70.7mm	Multifunctional curing agent	15%	2.72	3.73
40mm×40mm×160mm	Multifunctional curing agent		3.05	4.30
50mm×100mm	Multifunctional curing agent		2.45	3.52
70.7mm×70.7mm70.7mm	Multifunctional curing agent	20%	4.43	7.19
40mm×40mm×160mm	Multifunctional curing agent		4.92	8.20
50mm×100mm	Multifunctional curing agent		4.01	6.66
70.7mm×70.7mm70.7mm	cement	10%	0.80	1.31
40mm×40mm×160mm	cement		0.92	1.48
50mm×100mm	cement		0.75	1.19
70.7mm×70.7mm70.7mm	cement	15%	1.68	3.24
40mm×40mm×160mm	cement		1.9	3.63
50mm×100mm	cement		1.58	2.95
70.7mm×70.7mm70.7mm	cement	20%	3.22	3.77
40mm×40mm×160mm	cement		3.58	4.3
50mm×100mm	cement		2.88	3.44

3.5 Influence of Curing Agent Dosage on Self-Shrinkage Performance

The self-shrinkage of stabilized soil is due to the hydration reaction within the soil, which reduces moisture and subsequently causes volume contraction. Unlike dry shrinkage, self-shrinkage primarily occurs internally within the stabilized soil; even under sealed conditions, volume changes can still occur due to the depletion of internal moisture. As a material for the pile foundation of pressure-type composite anti-pull piles, high-strength fluidized stabilized soil has a shrinkage performance closely linked to the load-bearing capacity and durability of the pile.

The results of the self-shrinkage test for stabilized soil are shown in Figure 6. The test results indicate that the addition of a multi-component composite curing agent not only reduces shrinkage but also causes expansion when the dosage reaches 15%. As the cement content increases, the shrinkage rate of cement-flow stabilized soil gradually increases. The self-shrinkage rates for soils with 10%,15%, and 20% cement content are 429×10^-6, 648×10^-6, and 722×10^-6, respectively. The self-shrinkage rate increases threefold from 10% to 15%. With the increase in the dosage of the multi-component composite curing agent, the shrinkage of high-strength flow stabilized soil decreases. However, the overall trend is still a decrease in shrinkage for high-strength flow stabilized soil with 10% of the multi-component composite curing agent, although its shrinkage rate is lower than that of cement-soil at the same dosage. For high-strength flow stabilized soil with 15% of the composite curing agent, expansion occurs, with a self-shrinkage rate of-613×10^-6, which is twice lower than that of cement-soil at the same dosage.

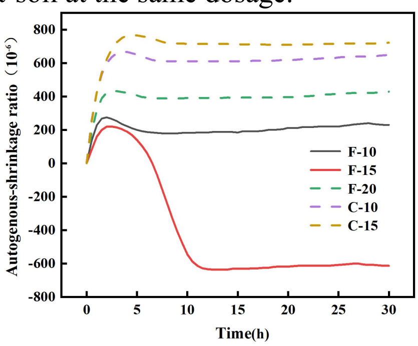

Figure 6. Self Shrinkage of Solidified Soil

3.6 Analysis of micro test results

3.6.1 Analysis of scanning electron microscope (SEM) results

This section mainly analyzes the scanning electron microscope results of cement soil with 15% mixing content and high strength fluid curing soil with 10%,15% and 20% mixing content, analyzes the influence of curing agent types and mixing content on the micro morphology of curing soil from the microscopic level, and expounds the mechanism of curing agent on redundant soil.

Figure 7 shows the scanning electron microscope (SEM) images of the cured soil samples after 28 days of curing. The high-strength fluid-cured soil produced a large amount of C-S-H gel and needle-like expansive hydration products, calcium sulfoaluminate (AFt), after 28 days of curing. These products effectively filled the pores and cracks in the soil, significantly enhancing its integrity. The amount of calcium sulfoaluminate generated increased gradually with the addition of composite curing agents. This phenomenon explains at the microscopic level why the self-shrinkage rate of high-strength fluid-cured soil decreases with the addition of multifunctional composite curing agents, which can reduce the shrinkage or even cause expansion of the cured soil.

The composite curing agent consists of slag, steel slag, desulfurization gypsum, and alkaline activators. These materials contain large amounts of CaO, Ca(OH)2, and active SiO2. When the composite curing agent is mixed with soil, the cementitious materials react through volcanic ash to form hydration products such as C-S-H. The addition of alkaline activators further increases the alkalinity of the system, promoting the full hydration of slag and steel slag, thereby enhancing later strength. Additionally, the CaSO4 in desulfurization gypsum promotes the formation of expansive hydration products, such as calcium sulfoaluminate, during the later stages of curing. These calcium sulfoaluminate hydrates effectively fill the pores and support adjacent soil particles. As gel hydration products continue to form, the structure of the cured soil becomes more compact, thus increasing its strength.

3.6.2 Analysis of mercury pressure test (MIP) results

Figure 8 shows the pore characteristics parameters of cured soil at 28 days when 15% cement and 10%,15%, and 20% composite curing agents were added. As can be seen from Figure 8, the porosity of high-strength fluid-cured soil with 10%,15%, and 20% curing agent additions is 37.98%,36.41%, and 33.65%, respectively. The porosity decreases gradually as the curing agent content increases, with the 20% addition yielding the lowest porosity. This is due to the highest slag content in the 20% addition, which results in the formation of the most hydrated calcium silicate gel. These reactants continuously fill the spaces between particles, leading to a gradual refinement of the pores in the cured soil. This also explains, at the microscopic level, why the strength of the cured soil increases with the addition of more composite curing agents. Observing Figure 8(a), it can be seen that compared to cement soil with a curing agent addition of 15%, the high-strength fluid-cured soil with the composite curing agent addition has a reduced pore volume at all pore sizes. This is the reason why the composite curing agent significantly enhances the strength of the cured soil.

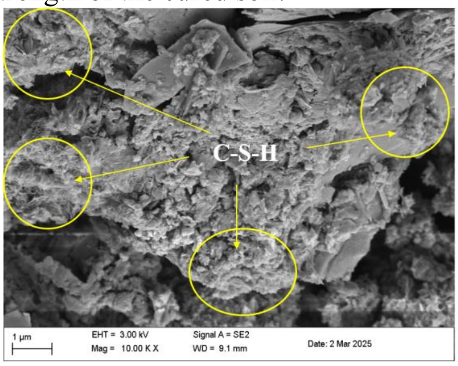

(a) Cement soil with 15% mixing

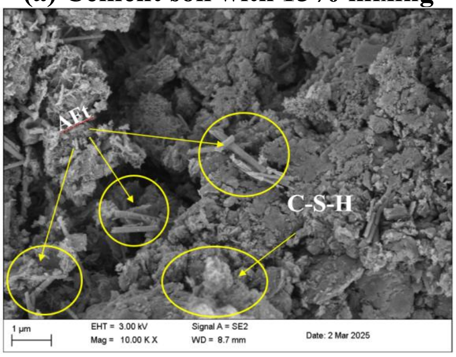

(b) 10% high strength fluid curing soil

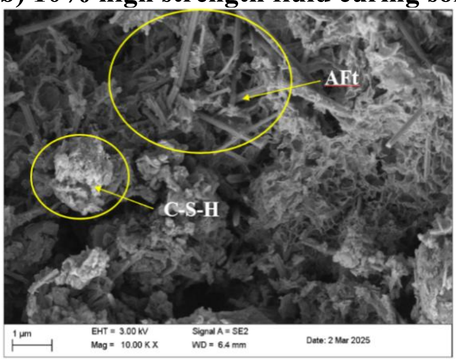

(c) 15% of the high strength fluid

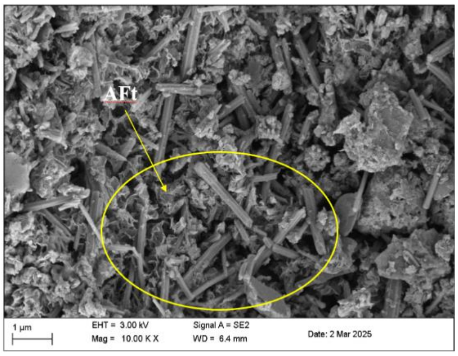

(d)20% of the high strength fluid

Figure 7. SEM Test Results of Solidified Soil

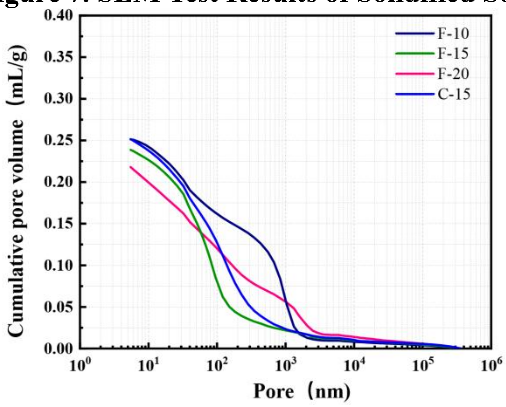

(a) Cumulative pore volume

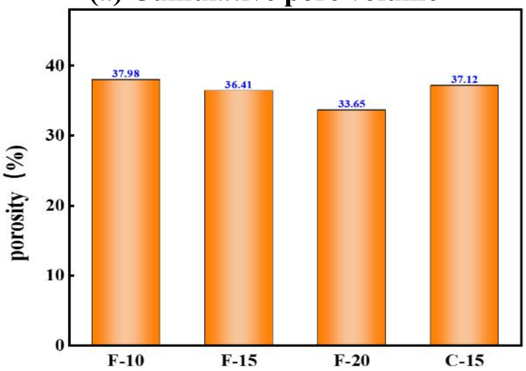

(b) porosity

Figure 8. MIP Test Results of Solidified Soil

4. Conclusion

In this paper, the multi-composite curing agent and P·O42.5 cement prepared from industrial solid wastes such as slag powder, steel slag powder and desulfurization gypsum are respectively mixed with redundant construction waste to prepare high strength fluid curing soil, and their mechanical properties and feasibility as pile foundation materials are studied, and the following conclusions are obtained:

(1) The optimal ratio of multiple composite curing agents is slag powder: steel slag powder: gypsum: alkaline activator =60:13:14:13, and the water-curing ratio is 0.32. The influence of water-curing ratio on flowability, 7d strength

and 28d strength is greater than that of gypsum content and lime content.

(2) The strength relationship of the three different specimens is: prism> cube> cylinder, in which the unconfined compressive strength of the 40mm × 40mm × 160mm prism is 1.1~1.15 times that of the 70.7mm×70.7mm×70.7mm cube, and the unconfined compressive strength of the 40mm × 40mm × 160mm prism is 1.2~1.25 times that of the 50mm × 100mm cylinder.

(3) The addition of polymeric composite curing agent can reduce the self-contraction of fluid curing soil. With the increase of the amount of polymeric composite curing agent, the shrinkage of high-strength fluid curing soil gradually decreases, and even produces a slight expansion effect when the amount reaches a certain amount.

(3) The addition of multiple composite curing agents leads to the formation of more C-S-H gel and expansive hydration product calcium aluminite in high strength fluid curing soil, which reduces the porosity and enhances the strength of the material.

References

[1] Zhou Yong. Discussion on buoyancy resistance of underground structures and emergency treatment measures [J]. Engineering and Construction, 2023,37(04):1190-1192.

[2] Yang Shujuan, Zhang Tongbo, Lu Tianqi, et al. Analysis and treatment measures of buoyancy resistance in basements [J]. Construction Technology, 2012,43(12):1067-1070.

[3] Wang Mei, Wu Jiong. Anti-floating design of underground engineering [J]. Building Structure, 2022,52(S2):2043-2046.

[4] Gao Xiaojuan, Dong Jiarong, Xie Lei, et al. Experimental study on the bearing mechanism model of pressure type anti-pull pile [J]. Journal of Henan University of Science and Technology (Natural Science Edition), 2023,44(06):63-69+8.

[5] Zhu Rui, Zhou Feng, Sheng Qiang, et al. Influence of cement content on shear characteristics of stiffened composite piles interface [J]. Journal of Nanjing Tech University (Natural Science Edition), 2023,45(05):546-553+562.

[6] Li Liye. Study on the Bearing Characteristics of Elastic Composite Piles [D]. Southeast University, 2016.

[7] Qian Yujun, Xu Zhiwei, Deng Yaguang, Sun Guimei. Engineering Application and Experimental Analysis of Elastic Composite Piles [J]. Journal of Geotechnical Engineering, 2013,35(S2):998-1001.

[8] Ping Dong, Ran Qin, Zhengzhou Chen. Bearing capacity and settlement of concrete-cored DCM pile in soft ground. 2004, 22(1):105-119.

[9] Tang Yixin, Liu Hanlong, Zhu Wei. Experimental study on engineering properties of cemented soil [J]. Journal of Geotechnical Engineering, 2000,22(5): 549-554.

[10] Lee F H, Lee Y, Chew S H, et al. Strength and modulus of marine clay-cement mixes[J]. Journal of Geotechnical and Geoenvironmental Engineering, 2005, 131(2): 178-186.

[11] Fischer K P, Andersen K H, Moum J. Properties of an artificially cemented clay[J]. Canadian Geotechnical Journal, 1978, 15(3): 322-331.

[12] Khattak M J, Alrashidi M. Durability and mechanistic characteristics of fiber reinforced soil–cement mixtures[J]. International Journal of Pavement Engineering, 2006, 7(1): 53-62.

[13] Zhou Yongxiang and Wang Jizhong. Principle and engineering application prospect of pre-mixed stabilized soil [J]. New Building Materials, 2019,46(10):117-120.

[14] Zhou Yongxiang, Huo Menghao, Hou Li, et al. Research status and prospect of low-intensity fluid fill materials [J]. Materials Bulletin, 2024,38(15):130-138.

[15] Amini O, Ghasemi M. Laboratory study of the effects of using magnesium slag on the geotechnical properties of cement stabilized soil[J]. Construction and Building Materials, 2019, 223: 409-420.

[16] Li Zhanguo, Zhao Yongsheng, Huang Xin. Discussion on the design method of solidifying agent for soft ground foundation prepared from industrial waste residue [J]. Journal of Beihang University, 2009,35(04):497-500.

[17] Li Yu, Hu Mingjian, Zheng Siwei, et al. Study on the Strength and Microscopic Mechanism of Calcined Expansive Soil with Calcium Carbide Slag and Mine Slag [J]. Rock and Soil Mechanics,

2024,45(S1):461-470.

[18] Wang Yingfu, Zhang Shuguang, Huang Xiao, et al. Study on Mechanical and Durability Properties of Phosphogypsum-Steel Dross-Slag Cured Low Liquid Limit Silty Clay [J]. Journal of Civil Engineering, 2023,56(S1):12-23.

[19] Tomohisa S, Sawa K, Naitoh N. Hedoro Hardening Treatment by Industrial Wastes[J]. Journal of the Society of Materials Science Japan, 1995, 44(503): 1023-1026.